

## TESTING THE GAUSSIAN RANDOM HYPOTHESIS WITH THE COSMIC MICROWAVE BACKGROUND TEMPERATURE ANISOTROPIES IN THE 3-YEAR WMAP DATA

LUNG-YIH CHIANG<sup>1</sup>, PAVEL D. NASELSKY<sup>1</sup>, PETER COLES<sup>2</sup>  
 chiang@nbi.dk, naselsky@nbi.dk, peter.coles@nottingham.ac.uk

*Submitted to the Astrophysical Journal Letter*

### ABSTRACT

We test the hypothesis that the temperature of the cosmic microwave background is consistent with a Gaussian random field defined on the celestial sphere, using de-biased internal linear combination (DILC) map produced from the 3-year WMAP data. We test the phases for spherical harmonic modes with  $\ell \leq 10$  (which should be the cleanest) for their uniformity, randomness, and correlation with those of the foreground templates. The phases themselves are consistent with a uniform distribution, but not for  $\ell \leq 5$ , and the differences between phases are not consistent with uniformity. For  $\ell = 3$  and  $\ell = 6$ , the phases of the CMB maps cross-correlate with the foregrounds, suggesting the presence of residual contamination in the DILC map even on these large scales. We also use a one-dimensional Fourier representation to assemble  $a_{\ell m}$  into the  $\Delta T_{\ell}(\varphi)$  for each  $\ell$  mode, and test the positions of the resulting maxima and minima for consistency with uniformity randomness on the unit circle. The results show significant departures at the 0.5% level, with the one-dimensional peaks being concentrated around the origin  $\varphi = 0$ . This strongly significant alignment with the Galactic meridian, together with the cross-correlation of DILC phases with the foreground maps, strongly suggests that even the lowest spherical harmonic modes in the map are significantly contaminated with foreground radiation.

*Subject headings:* cosmology: cosmic microwave background — cosmology: observations — methods: data analysis

### 1. INTRODUCTION

Since the release of the 1-year Wilkinson Microwave Anisotropy Probe (WMAP) data (Bennett et al. 2003b,c; Spergel et al. 2003; Hinshaw et al. 2003b; Komatsu et al. 2003), great efforts have been made to search and detect various possible forms of non-Gaussianity of the cosmic microwave background (CMB) temperature fluctuations (Chiang et al. 2003; Coles et al. 2004; Park 2004; Eriksen et al. 2004c; Vielva et al. 2004; Copi, Huterer & Starkman 2004; Cabella et al. 2004; Hansen et al. 2004; Mukherjee & Wang 2004; Larson & Wandelt 2004; Dineen & Coles 2006).

Three years of data are now available and methods of foreground cleaning have also been improved, so the WMAP team have produced a new ‘de-biased’ version of their internal linear combination map (henceforth the DILC), which is claimed to be suitable for analysis over the full sky for spherical harmonic modes up to  $\ell \leq 10$  (Spergel et al. 2006; Hinshaw et al. 2006). The statistics of these low multipole modes provide valuable information with cosmological significance, particularly concerning statistical isotropy (or lack of it), demonstrated by the CMB.

The 3-year data analyzed by the WMAP team is claimed to be Gaussian. Non-Gaussianity, if detected, could result from primordial origin (Bartolo et al. 2004), possible foreground residues left over after cleaning (Naselsky, Doroshkevich & Verkhodanov 2003, 2004; Dineen & Coles 2003; Naselsky & Novikov 2005), and/or correlated instrument noise. One will have to be very cautious if any non-Gaussianity is detected before attributing it to a primordial origin. The concept of internal linear combination

to obtain a reasonably clean CMB signal is to tune a set of weighting coefficients in order to minimize the variance of the foregrounds. Note that the variance is minimized but not eliminated. The possibility that foreground signals remain in the DILC map to a significant extent is therefore something that should be carefully tested.

In this paper we apply a series of stringent tests of the Gaussian hypothesis based on the behaviour of the phases of the spherical harmonic modes in the data. Since these phases are highly sensitive to the morphology (Chiang 2001) of the temperature pattern, comparison between the phases of the DILC and the derived foregrounds should give a sensitive indication of the presence of contamination. Phase information can also be used to diagnose departures from statistical homogeneity over the celestial sphere.

Using spherical harmonic phases in statistical tests involves some subtleties. For one thing, they are not rotationally invariant. In other words a different choice of  $z$ -axis leads to a different assignment of phases for the spherical harmonic modes of the same pattern. This can be dealt with in a number of ways (Coles et al. 2004), but in the present context we choose to fix our coordinate frame as that which makes most sense given the probable behaviour of the foregrounds. In all the following we assume a Galactic coordinate system; all phase information is interpreted relative to this preferred frame. In doing this we attempt to ensure that the detection of non-uniformity or non-randomness in the phases can be interpreted more simply in terms of Galactic foregrounds. Issues such as the claimed north-south asymmetry (Eriksen et al. 2004b) and the alignment of multipoles (Tegmark, de Oliveira-Costa

<sup>1</sup> Niels Bohr Institute, Blegdamsvej 17, DK-2100 Copenhagen, Denmark

<sup>2</sup> School of Physics & Astronomy, University of Nottingham, University Park, Nottingham NG7 2RD, United Kingdom

& Hamilton 2003; de Oliveira-Costa et al. 2004; Schwarz et al. 2004; Land & Magueijo 2005), which seem to persist in the WMAP 3-year data, are also measured in Galactic coordinates, so we hope to shed some additional light on these peculiarities.

Owing to the visual similarity of 1-year ILC and 3-year DILC maps, we will subject both maps to our analysis.

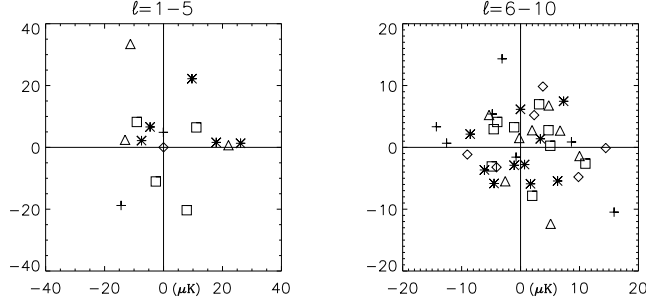


FIG. 1.— The  $a_{\ell m}$  for  $\ell \leq 10$  are plotted on the Argand plane. The amplitudes are in unit of  $\mu\text{K}$  and only  $m > 0$  modes are displayed. The signs  $\diamond$ ,  $+$ ,  $\triangle$ ,  $\square$  and  $*$  represent  $\ell = 1 - 5$  on the left,  $\ell = 6 - 10$  on the right panel, respectively. Note that 12 out of 15 phases of  $\ell \leq 5$  are in the first two quadrants, among which six are clustered near 0 or  $\pi$ .

## 2. THE GAUSSIAN RANDOM HYPOTHESIS AND THE CMB

The statistical characterization of CMB temperature anisotropies on a sphere can be expressed as a sum over spherical harmonics:

$$\Delta T(\theta, \varphi) = \sum_{\ell=0}^{\infty} \sum_{m=-\ell}^{\ell} a_{\ell m} Y_{\ell m}(\theta, \varphi), \quad (1)$$

where the  $Y_{\ell m}(\theta, \varphi)$  are spherical harmonic functions, defined in terms of the Legendre polynomials  $P_{\ell m}$  using

$$Y_{\ell m}(\theta, \varphi) = (-1)^m \sqrt{\frac{(2\ell + 1)(\ell - m)!}{4\pi(\ell + m)!}} P_{\ell m}(\cos \theta) \exp(im\varphi) \quad (2)$$

and the  $a_{\ell m}$  are complex coefficients which can be expressed with  $a_{\ell m} = |a_{\ell m}| \exp(i\phi_{\ell m})$ . In standard cosmological models (i.e. those involving the simplest forms of inflation) these fluctuations constitute a realization of a statistically homogeneous and isotropic Gaussian stochastic process, or random field, defined over the celestial sphere (Bardeen et al. 1986; Bond & Efstathiou 1987). The formal definition of such a Gaussian random field requires that the real and imaginary parts of the  $a_{\ell m}$  are independent and identically distributed according to a Gaussian probability density, so that the moduli  $|a_{\ell m}|$  have a Rayleigh distribution and the phases  $\phi_{\ell m}$  are uniformly random on the interval  $[0, 2\pi]$ . The Central Limit Theorem virtually guarantees that the superposition of a large number of harmonic modes will tend to a Gaussian as long as the phases are random, and this furnishes a weaker definition of Gaussianity. Moreover, statistical isotropy in general manifests itself in phase properties. Because of the importance of phases in both these definitions, we focus on their measured properties as probes of departures from Gaussianity. Many methods have been proposed to test the random phase hypothesis (Chiang, Coles & Naselsky 2002; Chiang, Naselsky & Coles 2004; Dineen, Rocha

and Coles 2005; Stannard & Coles 2005; Naselsky et al. 2004; Chiang & Naselsky 2006).

In Fig.1 we plot on the Argand plane the  $a_{\ell m}$  of the DILC map for  $\ell \leq 10$  (amplitudes  $|a_{\ell m}|$  in unit of  $\mu\text{K}$ ). Because of the conjugate properties of the  $a_{\ell m}$  for a real sky signal, we plot only  $a_{\ell m}$  modes with  $m \geq 1$  and omit all  $m = 0$  modes. Note the apparent non-uniformity of the phases for  $\ell \leq 5$ .

## 3. TESTING THE RANDOM PHASE HYPOTHESIS

We use Kuiper's statistic (Kuiper 1960) (KS) to test on the random phase hypothesis. The KS can be viewed as a variant of the standard Kolmogorov-Smirnov test, designed to cope with circular data. The standard Kolmogorov-Smirnov statistic is taken as the maximum distance of the cumulative probability distribution against the theoretical one:  $D = \max_{-\infty < x < \infty} |S_N(x) - P(x)|$ . For a circular function, however, one needs to take into account the maximum distance both above and below the theoretical probability  $P(x)$ . Accordingly, we define:  $D_{\pm} = \max_{-\infty < x < \infty} \pm(S_N(x) - P(x))$ . Then the test statistic is

$$V = D_{+} + D_{-}. \quad (3)$$

In standard frequentist fashion, we define the significance level  $\alpha$  (or  $p$ -value or “size”) for our “null” hypothesis (of uniform randomness of the phase angles) as the probability of the measured value of  $V$  arising under the null hypothesis. In this case,  $\alpha$  can be calculated from  $\alpha = Q_{\text{Kuiper}}(V[\sqrt{N} + 0.155 + 0.24/\sqrt{N}])$  and  $Q_{\text{Kuiper}}(\lambda) = 2 \sum_{j=1}^{\infty} (4j^2\lambda^2 - 1)e^{-2j^2\lambda^2}$ , where  $N$  is the number of data points.

We perform three statistical tests based on this general approach: on the *uniformity* of phases (i.e. consistency with a uniform distribution on the interval  $[0, 2\pi]$ ); on the *randomness* (i.e. independence) of phases by taking difference of phases with fixed separation ( $\Delta\ell, \Delta m$ ); and on the cross-correlation of each  $\ell$  between DILC and the foregrounds by  $\Delta\phi_{\ell m}^X = \phi_{\ell m}^{\text{dilc}} - \phi_{\ell m}^{\text{FG}}$ . In each case the resulting angles should be random: the difference between any two random angles is itself a random angle.

	$\phi_{\ell m}$ of $\ell \leq 5$	$\phi_{\ell m}$ of $6 \leq \ell \leq 10$	all $\phi_{\ell m}$ of $\ell \leq 10$
ILC	38.74%	90.91%	73.55%
DILC	30.63%	98.09%	66.14%

TABLE 1  
THE SIGNIFICANCE LEVEL  $\alpha$  IN ACCORD WITH THE UNIFORM DISTRIBUTION HYPOTHESIS OF THE PHASES OF THE 1-YEAR ILC AND 3-YEAR DILC MAPS.

We first test the uniformity of the phases for two groups ( $1 \leq \ell \leq 5$ ), and ( $6 \leq \ell \leq 10$ ) and for all phases claimed to describe clean modes (i.e.  $\ell \leq 10$ ). The phases of the  $m = 0$  modes are excluded in all our test. Table 1 shows that for the 3-year DILC, while the phases are consistent with a uniform distribution ( $\alpha \sim 0.98$ ) for  $6 \leq \ell \leq 10$ , and for  $\ell \leq 5$  ( $\alpha \sim 0.31$ ). This is consistent with the behaviour of the phases seen in Fig.1: the phases seem to be concentrated in the first two quadrants. This is however, only significant at the 31% level, which is barely  $1\sigma$ . Overall, therefore, the phases of the 3-year DILC map for  $\ell \leq 10$  are consistent with uniformity ( $\alpha = 0.66$ ).

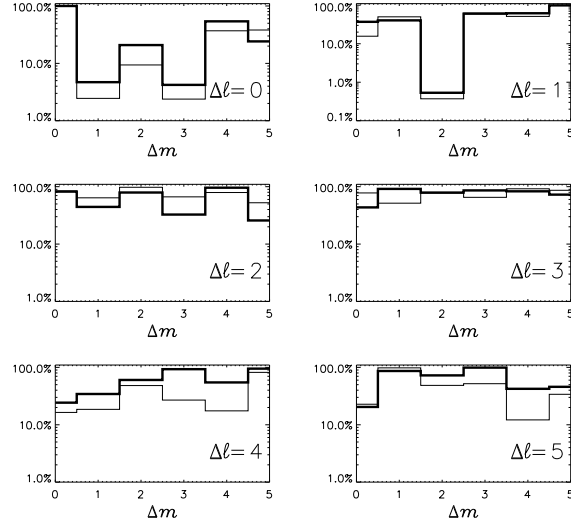


FIG. 2.— Significance levels of randomness with separation  $(\Delta\ell, \Delta m)$ . The thick and thin lines are from the 3-year DILC and 1-year ILC maps, respectively.

Now we check the randomness of the phases is tested by the defining a set of difference  $\Delta\phi^{\text{dilc}}(\Delta\ell, \Delta m) = \phi_{\ell+\Delta\ell, m+\Delta m}^{\text{dilc}} - \phi_{\ell m}^{\text{dilc}}$ . In Fig.2 we show the significance levels for randomness between phases with different  $\ell$  and  $m$ . There are three separations that show significant departures from uniformity ( $\alpha = 0.047, 0.0421$  and  $0.0053$  for  $(\Delta\ell, \Delta m) = (0, 1), (0, 3)$  and  $(1, 2)$ , respectively. This corresponds to significant coupling of the phases. It is complicated to understand coupling across both  $\ell$  and  $m$  for  $(\Delta\ell, \Delta m) = (1, 2)$  because of the lack of rotational invariance described earlier. Nevertheless, because the first two examples involve coupling between azimuthal numbers  $m$  within each  $\ell$ , we plot in Fig.3 the sequences of phase difference  $\Delta\phi^{\text{dilc}}(0, 1)$  and  $\Delta\phi^{\text{dilc}}(0, 3)$  on a unit circle (or  $\exp(i\Delta\phi^{\text{dilc}})$  on an Argand plane). For both distributions one can see the deficits around  $\Delta\phi = 0$  that cause the significance levels for the cases to appear below 5%. We also include  $(0, 2)$  in Fig.3 for comparison, which has the apparent tendency of phase differences to avoid  $\pi$ , though this is not significant at the 5% level.

#### 4. CROSS-CORRELATION BETWEEN THE DILC AND FOREGROUND MAPS

Since the DILC map is obtained from an internal combination of the frequency maps, some foreground residues might be left unsubtracted. Based on the assumption that CMB signal should not correlate with the foregrounds, and that the characteristic of phases reflect the morphology of the CMB anisotropy pattern, we also test the cross-correlation of phases for the DILC and the WMAP 3-year foreground maps at K, Ka, Q, V and W channels. The foreground maps we test are the sum of the synchrotron, free-free and dust templates. We take the phase difference  $\Delta\phi_{\ell m}^X = \phi_{\ell m}^{\text{dilc}} - \phi_{\ell m}^{\text{FG}}$  for each  $\ell$ , assuming such  $\Delta\phi_{\ell m}$  at each  $\ell$  should be uniformly distributed. In Fig.4 one can see that for  $\ell = 3$  and 6 the DILC phases have correlation with the foregrounds with significance around 10%. One particular point about the quadrupole is easily seen from Fig.1: two of the three quadrupole phases are near 0 and  $\pi$ . Note also that, for  $\ell = 6$ , in Fig.3 (shown in red diamond sign), the phase differences for  $\Delta m = 1$  are strongly

clustered.

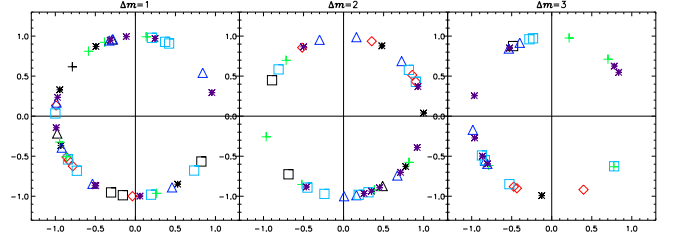


FIG. 3.— Phase difference for  $\Delta m = 1, 2$  and 3 for all  $\phi_{\ell m}^{\text{dilc}}, \ell \leq 10, 1 \leq m \leq \ell$  plotted on a unit circle. The significance levels of departures from uniformity are 4.70%, 20.85% and 4.21%, respectively. The signs  $\diamond, +, \triangle, \square$  and  $*$  in black represent phase difference within  $\ell = 1 - 5$ , respectively, and in color within  $\ell = 6 - 10$ , respectively.

#### 5. EXTREMA STATISTICS

The  $\Delta m$  phase coupling in each  $\ell$  leads to a departure from Gaussianity in the resulting signal. Following Chiang & Naselsky (2006) we represent the effect of phase coupling by assembling the  $a_{\ell m}$  (now only single variable  $m$ ) with an inverse Fourier transform:

$$\Delta T_{\ell}(\varphi) = \sum_m a_{\ell m}^{\text{dilc}} \exp(im\varphi), \quad (4)$$

where the negative  $m$  in the sum are replaced with  $a_{\ell m}^*$  to ensure that  $\Delta T_{\ell}$  is real. This one-dimensional Fourier representation is equivalent to using all the  $a_{\ell m}$  in the sum. The morphology of the signal obtained by this method is similar to the signal  $\Delta T(\phi, \varphi)$  obtained for each  $\ell$  by summing over all  $\theta$  onto  $\varphi$  direction. Such a construction obviously loses information in one of the available dimensions, but despite the fact that the  $a_{\ell m}$  are spherical harmonic coefficients, the statistics registered in the one-dimensional complex  $a_{\ell m}$  should still manifest themselves in the 1D  $\Delta T$  curves we create. In Fig.5 we plot  $\Delta T(\varphi)$  summing from the DILC  $a_{\ell m}$  (top), and from the whitened DILC:  $|a_{\ell m}/a_{\ell m}^*|$  (bottom). If the signal is Gaussian, the locations of the highest and lowest peaks should randomly distributed in  $\varphi$  between  $-180^\circ$  and  $180^\circ$ . We plot in Fig.6 the distribution of these extrema locations in a unit circle.

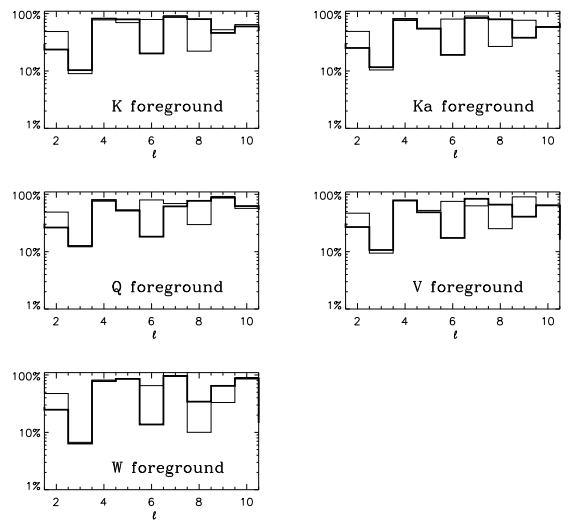


FIG. 4.— Significance levels for the cross-correlation of phases at each  $\ell$  between the DILC (thick lines) and the WMAP foreground maps, from top to bottom, K, Ka, Q, V and W channels, respectively. For comparison, the thin lines are those between 1-year ILC and 1-year foreground maps.

In Table 2 we list the significance of the distribution of the extrema locations. Not only do they show low significance levels of random distribution in  $\varphi$ , the peak locations also cluster in  $\varphi = 0$ . In Fig.4 the  $\ell = 3$  and 6 show significant cross correlation with the foregrounds. We therefore test the peak distribution by excluding the four extrema belonging to these two modes. Although  $p$ -values increase slightly, the results are still significant at a level below 5%.

	3-y DILC	Whitened 3-y DILC
all peaks $\ell \leq 10$	0.450%	0.552 %
excluding peaks of $\ell = 3, 6$	2.759%	4.218 %

TABLE 2

SIGNIFICANCE LEVELS OF THE UNIFORMITY OF THE DISTRIBUTION OF THE EXTREMA LOCATIONS IN  $T_\ell$ .

## 6. CONCLUSION

In this letter we test the Gaussian random hypothesis of the CMB temperature anisotropies. The behaviour of the 3-year DILC does not differ strongly from that of the 1-year ILC version: all the famous peculiarities still exist, as mentioned in Spergel et al. (2006). We have found in this paper that this also extends to the behaviour of the spherical harmonic phases. In particular, we find that phase differences (which should be uniformly distributed), tend to avoid the region of the complex plane close to  $\varphi = 0$ . We also find that the phases for  $\ell = 3$  and  $\ell = 6$  are significantly correlated with those of the foreground maps. We also test the real space alignment of the resulting features using the temperature extrema resulting from a Fourier summation for each  $\ell$ . The resulting peaks are indeed concentrated around the origin of Galactic coordinates, with respect to which the phases are themselves defined.

On the basis of these results we reject the null hypothesis that the modes with  $\ell \leq 10$  are a realization of a statistically homogeneous Gaussian random field at a significance level better than 5%. We also infer that the origin of the observed departures is consistent with being some form of Galactic foreground.

Of course it is possible the apparent alignment between CMB temperature pattern and galactic foreground morphology is simply fortuitous. It could be that large-scale anisotropies in both line up accidentally. If this is the case then we just happen to live at a place in the Universe where our past light cone presents us with this coincidence and we will just have to cope with it; all future diagnostics of foreground contamination will have to incorporate this alignment as conditioning information. We believe however that it is important to take such coincidences very seriously until we know for certain that is all they are.

<sup>3</sup> <http://www.eso.org/science/healpix/>

<sup>4</sup> <http://www.glesp.nbi.dk>

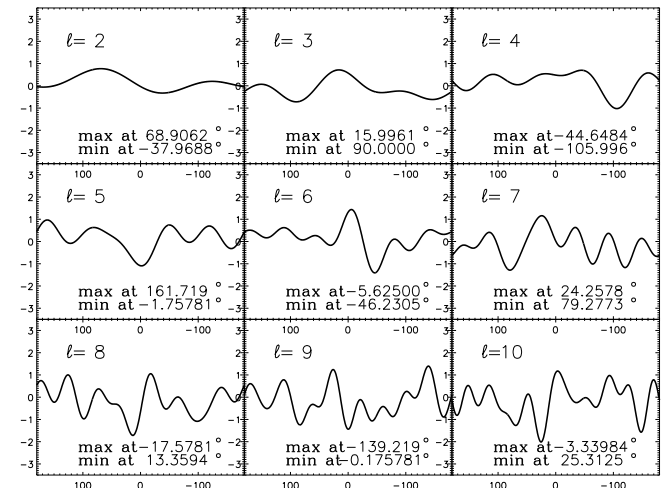
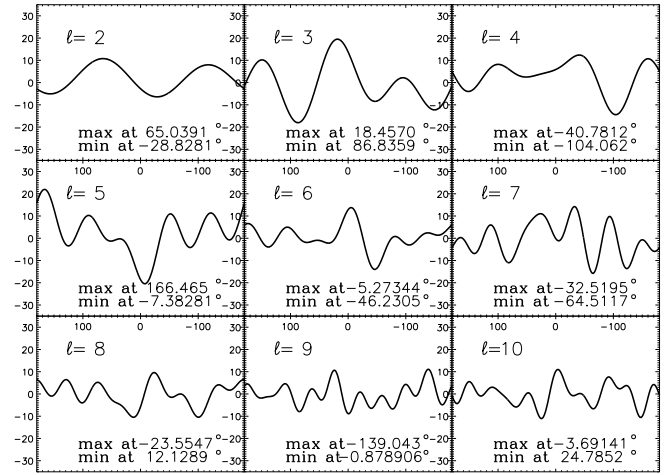


FIG. 5.— The  $\Delta T_\ell(\varphi)$  distribution for each  $\ell$  from the DILC map by assembling  $\sum_m a_{\ell m}^{\text{dilc}} \exp(im\varphi)$  (top panel, in which the unit of  $y$  axis is  $\mu\text{K}$ ) and by assembling only the phase part:  $\sum_m \exp(i\phi_{\ell m}^{\text{dilc}}) \exp(im\varphi)$  (bottom). In order to match the convention of Galactic longitude coordinates (for comparison with, e.g. Fig.14 in Hinshaw et al. (2006)), the  $\varphi$  axis is plotted reversely. In each figure we indicate the locations of the extrema.

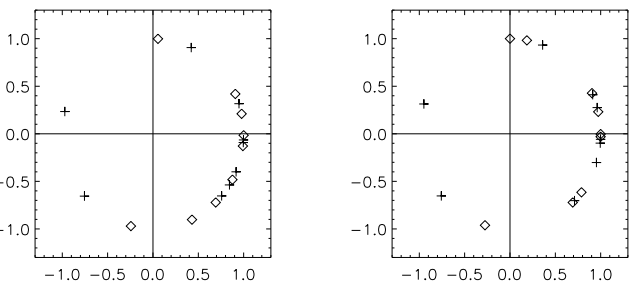


FIG. 6.— The distribution of the extrema locations of  $\Delta T_\ell(\varphi)$  as shown in Fig.5. The angle of the unit circle denotes the location  $\varphi$ . The left panel is for the DILC  $\Delta T_\ell(\varphi)$ , and the right for the whitened DILC  $\Delta T_\ell(\varphi)$ . The  $\diamond$  sign denotes maxima and the  $+$  sign minima.

## ACKNOWLEDGMENTS

We acknowledge the use of the NASA Legacy Archive for extracting the *WMAP* data. We also acknowledge the use of HEALPIX<sup>3</sup> package (Górski, Hivon & Wandelt 1999) to produce  $a_{\ell m}$  from the *WMAP* data and the use of GLESP<sup>4</sup> package (Doroshkevich et al. 2003).

## REFERENCES

Banday, A. J., Zaroubi, S., Gorski, K. M., 2000, *ApJ*, 533, 575  
 Bardeen, J. M., Bond, J. R., Kaiser, N., Szalay, A. S., 1986, *ApJ*, 304, 15  
 Bartolo, N., Komatsu, E., Matarrese, S., Riotto, A., 2004, *Phys. Rep.*, 402, 103  
 Bennett, C. L., et al., 2003, *ApJS*, 148, 1  
 Bennett, C. L., et al., 2003, *ApJS*, 148, 97  
 Bond, J. R., Efstathiou, G., 1987, *MNRAS*, 226, 655  
 Cabella, P., Hansen, F., Marinucci, D., Pagano, D., Vittorio, N., 2004, *Phys. Rev. D*, 69, 063007  
 Chiang, L.-Y., 2001, *MNRAS*, 325, 405  
 Chiang, L.-Y., Coles, P., 2000, *MNRAS*, 311, 809  
 Chiang, L.-Y., Coles, P., Naselsky, P. D., 2002, *MNRAS*, 337, 488  
 Chiang, L.-Y., Naselsky, P. D., Coles, P., 2004, *ApJL*, 602, 1  
 Chiang, L.-Y., Naselsky, P. D., Verkhodanov, O. V., Way, M. J., 2003, *ApJ*, 590, L65  
 Chiang, L.-Y., Naselsky, P. D., 2006, *Int. J. Mod. Phys. D* in press (astro-ph/0407395)  
 Coles, P., Barrow, J. D., 1987, *MNRAS*, 228, 407  
 Coles, P., Chiang, L.-Y., 2000, *Nature*, 406, 376  
 Coles, P., Dineen, P., Earl, J., Wright, D., 2004, *MNRAS*, 350, 989  
 Copi, C. J., Huterer, D., Starkman, G. D., 2004, *Phys. Rev. D*, 70, 043515  
 de Oliveira-Costa, A., Tegmark, M., Zaldarriaga, M., Hamilton, A., 2004, *Phys. Rev. D*, 69, 063516  
 Dineen, P., Coles, P., 2003, *MNRAS*, 347, 52  
 Dineen, P., Coles, P., 2006, *MNRAS* submitted (astro-ph/0511802)  
 Dineen, P., Rochar, G., Coles, P., 2005, *MNRAS*, 358, 1285  
 Doroshkevich, A. G., Naselsky, P. D., Verkhodanov, O. V., Novikov, D. I., Turchaninov, V. I., Novikov, I. D., Christensen, P. R., Chiang, L.-Y., 2003, *Int. J. Mod. Phys. D*, 14, 275  
 Eriksen, H. K., Hansen, F. K., Banday, A. J., Gorski, K. M., Lilje, P. B., 2004, *ApJ*, 605, 14  
 Eriksen, H. K., Novikov, D. I., Lilje, P. B., Banday, A. J., Gorski, K. M., 2004, *ApJ*, 612, 64  
 Ferreira, P., Magueijo, J., Gorski, K. M., 1998, *ApJ*, 503, L1  
 Gaztanagz, E., Wagg, J., 2003, *Phys. Rev. D*, 68, 021302  
 Gorski, K. M., Hivon, E., Wandelt, B. D., 1999, in A. J. Banday, R. S. Sheth and L. Da Costa, *Proceedings of the MPA/ESO Cosmology Conference “Evolution of Large-Scale Structure”*, PrintPartners Ipskamp, NL  
 Hansen, F. K., Cabella, P., Marinucci, D., Vittorio, N., 2004, *ApJL*, 607, 67  
 Hinshaw, G., et al., 2003, *ApJS*, 148, 135  
 Hinshaw, G., et al., 2006, *ApJ* (astro-ph/0603451)  
 Komatsu, E., et al., 2003, *ApJS*, 148, 119  
 Kuiper, N. H., 1960, *Proceedings of the Koninklijke Nederlandse Akademie van Wetenschappen, Series A*, Vol 63  
 Land, K., Jagueijo, J., 2005, *Phys. Rev. Lett.*, 95, 071301  
 Larson, D. L., Wandelt, B. D., 2004, *ApJL*, 613, 85  
 Matsubara, T., 2003, *ApJL*, 591, 79  
 Mukherjee, P., Wang, Y., 2004, *ApJ*, 613, 51  
 Naselsky, P. D., Chiang, L.-Y., Verkhodanov, O. V., Novikov, I. D., 2005, *Int. J. Mod. Phys. D*, 14, 1273  
 Naselsky, P. D., Chiang, L.-Y., Olesen, P., Novikov, I. D., 2005, *Phys. Rev. D*, 72, 3512  
 Naselsky, P. D., Doroshkevich, A., Verkhodanov, O. V., 2003, *ApJL*, 599, 53  
 Naselsky, P. D., Doroshkevich, A., Verkhodanov, O. V., 2004, *MNRAS* 349 695 (astro-ph/0310601)  
 Naselsky, P. D., Novikov, I. D., 2005, *Int. J. Mod. Phys. D*, 10, 1769  
 Park, C.-G., 2004, *MNRAS*, 349, 313  
 Schwarz, D. J., Starkman, G. D., Huterer, D., Copi, C. J., 2004, *Phys. Rev. Lett.*, 93, 221301  
 Spergel, D. N., et al., 2006, *ApJ* submitted (astro-ph/0603449)  
 Spergel, D. N., et al., 2003, *ApJS*, 148, 175  
 Stannard, A., Coles, P., 2005, *MNRAS*, 364, 929  
 Tegmark, M., de Oliveira-Costa, A., Hamilton, A., 2003, *Phys. Rev. D*, 68, 123523  
 Vielva, P., Martinez-Gonzalez, E., Barreiro, R. B., Sanz, J. L., Cayon, L., 2004, *ApJ*, 609, 22